

Stark shifts and fine structure of the ${}^6\text{Li } 3^2\text{D}_{3/2,5/2}$ states

R. Ashby, J.J. Clarke, and W.A. van Wijngaarden^a

Physics Department, Petrie Bldg., York University, 4700 Keele St. Toronto, Ontario, Canada M3J 1P3

Received 26 September 2002 / Received in final form 22 January 2003

Published online 11 March 2003 – © EDP Sciences, Società Italiana di Fisica, Springer-Verlag 2003

Abstract. ${}^6\text{Li } 3^2\text{D}_{3/2,5/2}$ states were studied using a diode laser to first excite the $2\text{P}_{3/2}$ state and a dye laser to populate the $3^2\text{D}_{3/2,5/2}$ states. The dye laser was modulated by an electro-optic modulator and intersected an atomic beam that passed through a field free region and subsequently through a uniform electric field. A value of 1084.24 ± 0.20 MHz was found for the 3^2D fine structure splitting. The scalar and tensor polarizabilities were determined to be $\alpha_0(3\text{D}_{3/2}) = -3.753 \pm 0.015$, $\alpha_2(3\text{D}_{3/2}) = 2.893 \pm 0.017$, $\alpha_0(3\text{D}_{5/2}) = -3.772 \pm 0.008$ and $\alpha_2(3\text{D}_{5/2}) = 4.058 \pm 0.013$ MHz/(kV/cm)².

PACS. 32.10.Fn Fine and hyperfine structure – 32.60.+i Zeeman and Stark effects

1 Introduction

Recently developed techniques permit the precision measurement of Stark shifts and fine structure splittings which are important for testing our understanding of atomic models [1,2]. These experiments yield data that are substantially more accurate than measurements of lifetimes or oscillator strengths and therefore stringently test theory. Lithium is the simplest alkali atom to model as it has only 3 electrons. Significant advances have been made computing the nonrelativistic energies of two electron atomic systems using the so-called Hylleraas variational technique during the last decade [3]. The extension of this work to neutral lithium is in progress [4]. It is important to compare theoretical calculations of atomic properties such as fine structure splittings and polarizabilities with precise measurements. This in turn will permit neutral lithium to be a testing ground for QED [5–7]. The understanding of the lithium atom is also necessary to probe the nuclear structure [8,9]. Indeed, the radioactive isotope ${}^7\text{Li}$ is predicted to have two so called halo neutrons that should be observed by precisely measuring the D line isotope shift [10].

The 3^2D fine structure splitting has been measured by a variety of experimental techniques [11–16]. The two most accurate determinations have uncertainties of 0.33 and 0.06 MHz but disagree by over 6 times the largest of the two uncertainties [11,12]. The resolution of this discrepancy is important as the 3^2D fine structure interval has been used to calibrate fine structure measurements of higher lithium states [17].

Comparatively little work has been done studying the Stark shifts of transitions in lithium except for the D lines

[21–23]. The $3^2\text{D}_{3/2,5/2}$ polarizabilities of lithium have never before been measured. The response of an atomic D state to an electric field \mathcal{E} is given by the following Hamiltonian [18]

$$H = a\mathbf{L} \cdot \mathbf{S} - \left\{ \alpha_0 + \alpha_2 \frac{3L_z^2 - \mathbf{L}^2}{L(2L-1)} \right\} \frac{\mathcal{E}^2}{2}. \quad (1)$$

Here, a is the fine structure coupling constant, \mathbf{L} is the electronic orbital angular momentum, \mathbf{S} is the electron spin while α_0 and α_2 are the scalar and tensor polarizabilities respectively. The term proportional to α_2 vanishes when $L = 0, 1/2$. The eigenenergies for the atomic D state are as follows

$$\begin{aligned} E(\text{D}_{5/2}, |m_J| = 5/2) &= a + x_1 \\ E(\text{D}_{5/2}, |m_J| = 3/2) &= -\frac{a}{4} + \frac{x_1 + x_2}{2} \\ &\quad + \frac{1}{2} \left[\frac{25}{4} a^2 - 3a(x_1 - x_2) + (x_1 - x_2)^2 \right]^{1/2} \\ E(\text{D}_{5/2}, |m_J| = 1/2) &= -\frac{a}{4} + \frac{x_2 + x_3}{2} \\ &\quad + \frac{1}{2} \left[\frac{25}{4} a^2 + a(x_3 - x_2) + (x_3 - x_2)^2 \right]^{1/2} \\ E(\text{D}_{3/2}, |m_J| = 3/2) &= -\frac{a}{4} + \frac{x_1 + x_2}{2} \\ &\quad - \frac{1}{2} \left[\frac{25}{4} a^2 - 3a(x_1 - x_2) + (x_1 - x_2)^2 \right]^{1/2} \\ E(\text{D}_{3/2}, |m_J| = 1/2) &= -\frac{a}{4} + \frac{x_2 + x_3}{2} \\ &\quad - \frac{1}{2} \left[\frac{25}{4} a^2 + a(x_3 - x_2) + (x_3 - x_2)^2 \right]^{1/2}. \quad (2) \end{aligned}$$

Here, $x_1 = -\frac{1}{2}(\alpha_0 + \alpha_2)\mathcal{E}^2$, $x_2 = -\frac{1}{2}(\alpha_0 - \alpha_2/2)\mathcal{E}^2$ and $x_3 = -\frac{1}{2}(\alpha_0 - \alpha_2)\mathcal{E}^2$. The scalar polarizability α_0 equals

^a e-mail: wlasery@yorku.ca

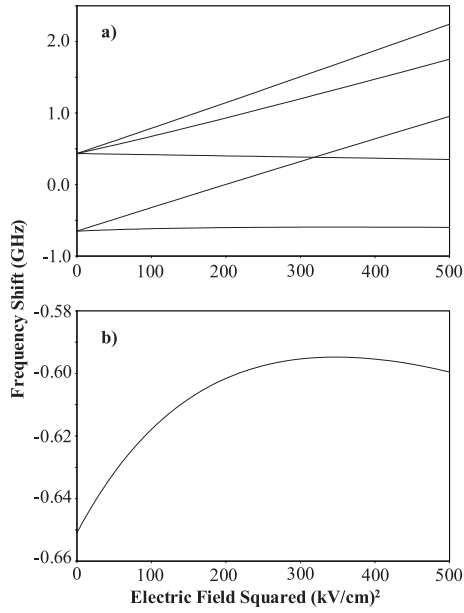


Fig. 1. Computed Stark shift of the Li $3^2D_{3/2,5/2}$ states. (a) The upper $3D_{5/2}$ state splits into three eigenstates determined by the absolute value of the magnetic sublevel quantum number $|m_J|$ while the lower $3D_{3/2}$ state splits into two eigenstates. The Stark shift has a quadratic dependence on the electric field where it is not influenced by the fine structure mixing. This influence is most evident in (b) for the $3D_{3/2}$ $|m_J| = 3/2$ state.

that of either the $D_{3/2}$ or $D_{5/2}$ state while the tensor polarizability is related to that of the $D_{3/2,5/2}$ states *via* the relation $\alpha_2 = \alpha_2(D_{5/2}) = \frac{10}{7}\alpha_2(D_{3/2})$. The eigenstates have been labelled using the azimuthal quantum number m_J corresponding to the total electronic angular momentum J which is a valid quantum number only in the limit of small electric fields.

The eigenenergies given by equation (2) are plotted *versus* the square of the electric field in Figure 1. Here, the value of 1084 MHz was used for the 3^2D fine structure splitting along with the theoretical estimates of $\alpha_0 = -3.76$ and $\alpha_2 = 4.09$ MHz/(kV/cm)² for the scalar and tensor polarizabilities as determined using a Coulomb approximation [19,20]. The latter approximates the potential experienced by the single valence electron by a Coulomb potential exerted by the nucleus and inner shell electrons. The eigenenergies have an approximately linear dependence on the square of the electric field. However, the $3D_{3/2}$ $|m_J| = 3/2$ state has a highly nonlinear dependence on the square of the electric field due to Stark mixing of the fine structure states, as is shown in Figure 1b.

2 Experiment

The apparatus has been described elsewhere and is therefore only briefly illustrated in Figure 2 [2]. An atomic beam was generated by heating a sample of ^6Li to 450 °C. Atoms were collimated using a series of slits generating

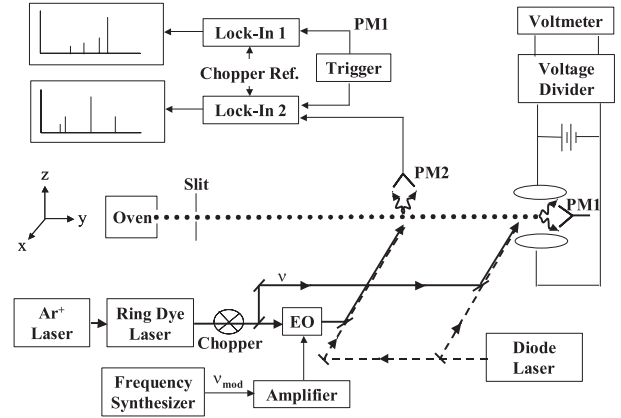


Fig. 2. Experimental setup. See text for description.

a beam having a divergence of about 1 milliradian. The atoms passed through a field free region and subsequently through a uniform electric field generated by two circular stainless steel plates having a diameter of 7.62 cm. A diode laser (Tuioptics DL100) generated a 1–2 mW laser beam that excited the $2S_{1/2}$ ($F = 3/2$) hyperfine level to the $2P_{3/2}$ state. A narrow linewidth (≈ 0.5 MHz) dye laser (Coherent 699) was then scanned across the $2P_{3/2} \rightarrow 3^2D_{3/2,5/2}$ resonance. The dye laser beam passed through an electro-optic modulator (EO) that generated frequency sidebands. Fluorescence was detected using two photomultipliers (PM1 & PM2) and their signals were analyzed by two lock-in amplifiers.

A sample signal consisted of about 12000 points and is shown in Figure 3. The two smaller $3D_{5/2}$ peaks in Figure 3a were generated by the laser sidebands electro-optically shifted by $\nu_{\text{mod}} = 995.000$ MHz. The center of each peak was found by fitting a Gaussian function, using the internal curve fitting function of the lock-in amplifier. The lock-in was unable to fit a Lorentzian function which best models an atomic transition's natural lineshape where Doppler broadening is negligible. The difference in the peak center values resulting from a Gaussian or a Lorentzian fit to the data was found to be negligible. The fullwidth at half maximum intensity (FWHM) of each peak was found to be approximately equal to the 16.8 MHz natural transition linewidth. Each laser frequency scan was separately calibrated.

The closely spaced $3D_{3/2}$ and $3D_{5/2}$ peaks were modelled using two Lorentzian functions. Either of the peak centers shifted less than 0.1 MHz when only one of these closely spaced peaks was fitted. The 3^2D fine structure splitting was determined by measuring the interval separating the $3D_{3/2}$ peak from the nearest $3D_{5/2}$ peak and adding ν_{mod} . Table 1 lists the results of 11 separate days of data runs. The uncertainty of each day's result is the error in the average due to the standard deviation of the data about the average value.

The Stark shift was measured using an unmodulated dye laser beam to excite the atoms as they passed between two field plates separated by 1.0163 ± 0.0003 cm. The electric field was generated using a high voltage power supply

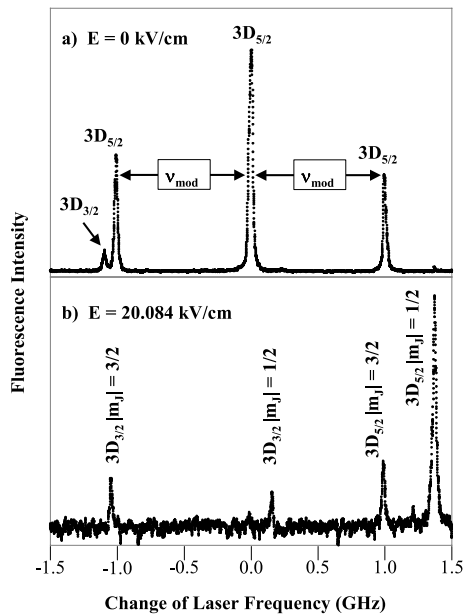


Fig. 3. Sample fluorescence signal resulting from a dye laser scan. Figure (a) shows the signal observed in the field free region where the largest $3\text{D}_{5/2}$ peak was generated using the unshifted dye laser frequency. The other two $3\text{D}_{5/2}$ peaks were generated by the frequency sidebands of the dye laser shifted by $\nu_{\text{mod}} = 995.000$ MHz. These two peaks as well as the $3\text{D}_{3/2}$ peak have been magnified by a factor of two in this figure. Figure (b) shows the signal observed simultaneously as in (a), when the atoms passed through an electric field of 20.084 kV/cm.

Table 1. Measurement of 3^2D fine structure.

Data set	Number of scans	Result (MHz)
1	73	$1\,084.55 \pm 0.48$
2	38	$1\,085.18 \pm 0.60$
3	53	$1\,083.54 \pm 0.74$
4	33	$1\,084.15 \pm 0.76$
5	30	$1\,082.40 \pm 1.09$
6	27	$1\,083.77 \pm 0.62$
7	22	$1\,085.56 \pm 0.92$
8	43	$1\,083.49 \pm 0.62$
9	23	$1\,085.51 \pm 0.99$
10	51	$1\,084.02 \pm 0.51$
11	46	$1\,084.35 \pm 0.86$
Average		$1\,084.24 \pm 0.20$

that had a ripple of less than 0.03%. The voltage was determined using a precision voltage divider (1/5 000) and a voltmeter. Figure 3b shows the $3^2\text{D}_{3/2,5/2} |m_J| = 1/2, 3/2$ fluorescence peaks shifted by an applied electric field of 20.084 kV/cm.

The $3\text{D}_{5/2}$ Stark shift was examined as follows. Figure 4 shows a plot of the frequency interval separating the $3\text{D}_{5/2} |m_J| = 3/2$ peak as observed in the field region and the $3\text{D}_{5/2}$ peak excited by the laser sideband in the field free region as a function of the electric field. A line was

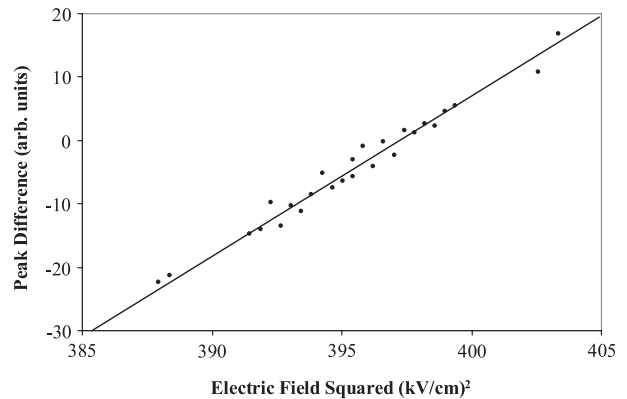


Fig. 4. Stark shift data of $3\text{D}_{5/2} |m_J| = 3/2$ state. The laser was scanned across the resonance and the electric field was varied to determine the field strength such that the $3\text{D}_{5/2}$ peak excited in the field free region by the laser frequency sideband shifted by 995.000 MHz was simultaneously excited as the $3\text{D}_{5/2} |m_J| = 3/2$ peak in the field region. The electric field needed to overlap the two peaks was found using a linear fit to be 19.611 ± 0.008 kV/cm.

fit to the data to determine the electric field giving a zero peak difference. This procedure for finding the Stark shift was repeated for the $3\text{D}_{5/2} |m_J| = 1/2$ peak.

An important experimental check is to measure the overlap of the various peaks when no voltage is applied to the field plates. A small offset ν_{off} was found resulting from the small difference in intersection angles between the laser and atomic beams in the field free and field regions. The actual Stark shift of the $2\text{P}_{3/2} \rightarrow 3\text{D}_J$ transition was therefore given by $\nu_{\text{mod}} + \nu_{\text{off}}$ which equalled the energy separating the upper and lower atomic states

$$\nu_{\text{mod}} + \nu_{\text{off}} = E(3\text{D}_J, |m_J|) - E(2\text{P}_{3/2}, |m_J| = 3/2). \quad (3)$$

Two equations corresponding to equation (3) for the $3\text{D}_{5/2} |m_J| = 1/2, 3/2$ states depend nonlinearly on the polarizabilities α_0 and α_2 . These equations were solved using the Excel Solver feature. The Stark shift of the $2\text{P}_{3/2}$ state has been studied, giving values of $\alpha_0(2\text{P}_{3/2}) = 31.63 \pm 0.17$ kHz/(kV/cm) 2 and $\alpha_2(2\text{P}_{3/2}) = 0.406 \pm 0.011$ kHz/(kV/cm) 2 [22, 23].

The $3\text{D}_{3/2} |m_J| = 3/2$ Stark shift was examined in a manner similar to that described above for the $3\text{D}_{5/2} |m_J| = 1/2, 3/2$ sublevels. The only difference is that due to the small size of the $3\text{D}_{3/2}$ fluorescence peak, corresponding peaks generated by the laser sidebands were not readily observed. Therefore, the electric field necessary to shift the $3\text{D}_{3/2} |m_J| = 1/2$ peak such that it was excited in the field region simultaneously as the $3\text{D}_{5/2}$ peak excited by the unmodulated laser beam in the field free region, was measured.

The electric field required to produce a 1 GHz Stark shift of the $3\text{D}_{3/2} |m_J| = 3/2$ peak exceeds 80 kV/cm, which was beyond the capability of available power supplies. Instead, the Stark shift was measured at electric fields below 12 kV/cm as shown in Figure 5. A function $y = A_0\mathcal{E}^2 + A_1\mathcal{E}^4$ was fit to the data yielding

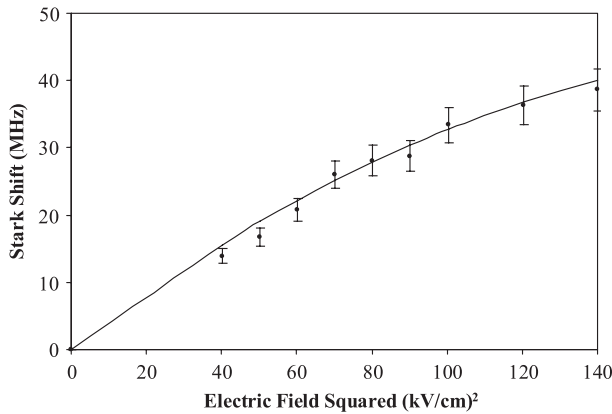


Fig. 5. Sample stark shift data of $3D_{3/2}|m_J| = 3/2$ state. The data was fitted to a curve $y = A_0\mathcal{E}^2 + A_1\mathcal{E}^4$ as described in the text.

Table 2. Polarizabilities of lithium $3^2D_{3/2,5/2}$ states in units of MHz/(kV/cm)².

Quantity	Experiment	Theory [20]
$\alpha_0(3D_{3/2})$	-3.753 ± 0.015	-3.74
$\alpha_2(3D_{3/2})$	2.893 ± 0.017	2.86
$\alpha_0(3D_{5/2})$	-3.772 ± 0.008	-3.76
$\alpha_2(3D_{5/2})$	4.058 ± 0.013	4.09

$A_0 = 0.430 \pm 0.016$ MHz/(kV/cm)² and $A_1 = -0.0010 \pm 0.0001$ MHz/(kV/cm)⁴. From equation (2), this result equals the following expression

$$-\frac{1}{2}[\alpha_0(3D_{3/2}) + \alpha_2(3D_{3/2})] = 0.430 \pm 0.016 \text{ MHz}/(\text{kV}/\text{cm})^2. \quad (4)$$

The $3D_{3/2}$ scalar and tensor polarizabilities were determined using equations (3, 4). Table 2 lists the polarizabilities where the errors were found by adding the various uncertainties due to the determination of the plate spacing, voltage divider, determination of ν_{off} etc. in quadrature.

3 Discussion of results

The result for the 3^2D fine structure splitting is compared to the best existing measurements in Table 3. The most accurate experiments used the level crossing and Doppler-free 2 photon techniques [11,12]. Our measurement agrees with the most accurate Doppler-free 2 photon result but strongly disagrees with the earlier level crossing result.

The level crossing experiment by Smith and Eck [11] was done in a vapor cell where an electric discharge excited the $3^2D_{3/2,5/2}$ states. A magnetic field was applied to the cell which shifted the hyperfine levels of these states. Fluorescence was monitored as a function of the magnetic field and was significantly perturbed at certain field strengths where two hyperfine levels “cross”. This enabled the fine

Table 3. Comparison of 3^2D fine structure measurements. MCHF stands for a Multiconfigurational Hartree-Fock calculation.

Technique	Result (MHz)	Reference
Level crossing	1081.69 ± 0.33	[11]
2 step laser excitation	1074 ± 3.0	[13]
Doppler-free 2 photon	1083.7 ± 2.0	[14]
Level crossing	1080.1 ± 1.0	[15]
Doppler-free 2 photon	1083.94 ± 0.06	[12]
Theory (MCHF)	1079	[26]
This work	1084.24 ± 0.20	

structure splitting to be determined. The largest uncertainty arose due to limitations of the curve fitting procedure.

The Doppler-free two photon experiment by Burghardt *et al.* [12] excited the $3D_{3/2}$ or $3D_{5/2}$ state directly from the ground state of a ^7Li atomic beam using two photons from a single CW dye laser beam. The dye laser frequency was stabilized using a reference cavity whose length was locked using the electro-optically modulated sideband of a HeNe laser beam. The HeNe laser frequency was in turn locked to an iodine absorption line. Hence, the dye laser frequency could be tuned by adjusting the EO modulation frequency. A photomultiplier detected fluorescence generated by the radiative decay of the $3^2D_{3/2,5/2}$ states to the $2P$ state. The integrated fluorescence signal was plotted as a function of the modulation frequency for each of the four $2S_{1/2}(F) \rightarrow 3^2D_{3/2,5/2}$ transitions, where $F = 1, 2$ are the hyperfine levels of the ground state. These four transition frequencies depend on the 3^2D fine structure interval, as well as on the hyperfine splittings of the $2S_{1/2}$ and the $3^2D_{3/2,5/2}$ states, which were then determined.

A difficulty in measuring the 3^2D fine structure splitting is that the hyperfine level splitting of the $^{6,7}\text{Li}$ $3^2D_{3/2,5/2}$ states is less than the natural linewidth of the 3^2D state. Therefore, it is not straightforward to excite a single $3^2D_{3/2,5/2}$ hyperfine level and then apply a correction for the shift of each of these hyperfine levels relative to the center of gravity of either the $3D_{3/2}$ or $3D_{5/2}$ state to obtain the 3^2D fine structure splitting. Our experiment studied ^6Li because its nuclear magnetic moment is 25% of that for ^7Li [24], resulting in much smaller hyperfine splittings. The laser predominantly excited the $2P_{3/2}(F = 3/2)$ level to the $3D_{3/2}(F = 5/2)$ and $3D_{5/2}(F = 7/2)$ hyperfine levels which have the strongest transition probabilities. The ^6Li $3^2D_{3/2,5/2}$ magnetic dipole hyperfine constants were estimated using theoretical calculations made for ^7Li [25] that agree with experimental measurements [12]. This resulted in a correction of +0.16 MHz to be applied to our fine structure result listed in Table 3. This is smaller than our experimental uncertainty and was thus neglected. The Burghardt group did account for the ^7Li $3^2D_{3/2,5/2}$ hyperfine structure, but it is not apparent whether the level crossing experiment of Smith and Eck considered this effect.

The only existing theoretical calculation of the lithium 3^2D fine structure value was found by Fröse Fischer *et al.* [26], using multiconfigurational Hartree-Fock variational calculations, and is listed in Table 3. This value disagrees with the best experimental values. The likely reason for this discrepancy is that quantum electrodynamic (QED) effects were not accounted for.

Table 2 compares the experimentally measured polarizabilities with those found using a Coulomb approximation. The latter technique has been found to be valid to within 2% for states of other alkali atoms excluding the lowest P states [1,2], which implies that this is a well established technique for measuring the scalar and tensor polarizabilities of alkali atoms. The present results are all within 1.5% of the theoretical values illustrating the utility of the Coulomb approximation method for calculating scalar and tensor polarizabilities of Li states where no experimental data exists. The precision of these results should encourage more refined theoretical calculations or comparative experiments, since no other measurements of the polarizabilities of the lithium $3^2\text{D}_{3/2,5/2}$ states exist. In particular, it would be of interest to determine whether the wavefunctions obtained using the Hylleraas variational technique to determine the nonrelativistic state energies can be used to accurately predict polarizabilities.

The authors wish to thank the Natural Science and Engineering Research Council of Canada and the Canadian Institute for Photonic Innovations for financial support. One of us, J.J. Clarke, is the recipient of an OGS and a JDS Uniphase scholarship.

References

1. W. van Wijngaarden, *Adv. At. Mol. Opt. Phys.* **36**, 141 (1996)
2. W. van Wijngaarden, *At. Phys.* **16**, 305 (1999)
3. G. Drake, *Atomic, Molecular & Optical Physics Handbook*, edited by G. Drake (AIP, New York, 1996)
4. Z. Yan, M. Tambasco, G. Drake, *Phys. Rev. A* **57**, 1652 (1998)
5. E. Riis, A. Sinclair, O. Poulsen, G. Drake, W. Rowley, A. Levick, *Phys. Rev. A* **49**, 207 (1994)
6. H. Rong, S. Grafström, J. Kowalski, R. Neumann, G. zu Putlitz, *Opt. Commun.* **201**, 345 (2002)
7. J. Clarke, W. van Wijngaarden, *Recent Research Developments in Physics* (Transworld Research Network, 2003, to be published)
8. Z. Yan, G. Drake, *Phys. Rev. A* **61**, 22504-1 (2000)
9. Z. Yan, G. Drake, submitted for publication (2002)
10. F. Schmitt, A. Dax, R. Kirchner, H. Kluge, T. Kühn, I. Tanihata, M. Wakasugi, H. Wang, C. Zimmermann, *Hyperf. Interact.* **127**, 111 (2000)
11. R. Smith, T. Eck, *Phys. Rev. A* **2**, 2179 (1970)
12. B. Burghardt, B. Hoffmann, G. Meisel, *Z. Phys. D* **8**, 109 (1988)
13. W. Hartig, V. Wilke, H. Walther, *Opt. Commun.* **14**, 244 (1975)
14. J. Kowalski, R. Neumann, H. Suhr, K. Winkler, G. zu Putlitz, *Z. Phys. A* **287**, 247 (1978)
15. R. Champeau, G. Leuchs, H. Walther, *Z. Phys. A* **288**, 323 (1978)
16. L. Radziemski, R. Engleman, J. Brault, *Phys. Rev. A* **52**, 4462 (1995)
17. J. Wangler, L. Henke, W. Wittmann, H. Plöhn, H. Andrä, *Z. Phys. A* **299**, 23 (1981)
18. A. Khadjavi, A. Lurio, W. Happer, *Phys. Rev.* **167**, 128 (1968)
19. D. Bates, A. Damgaard, *Philos. Trans. R. Soc. Lond. A* **242**, 101, (1949)
20. R. Ashby, W. van Wijngaarden, *J. Quant. Spect. Rad. Trans.* **76**, 467, (2003)
21. L. Hunter, D. Krause, D. Berkeland, M. Boshier, *Phys. Rev. A* **44**, 6140 (1991)
22. L. Windholz, M. Musso, G. Zerza, H. Jäger, *Phys. Rev. A* **46**, 5812 (1992)
23. J. Pipin, D. Bishop, *Phys. Rev. A* **47**, R4571 (1993)
24. D.R. Lide, *Handbook of Chemistry and Physics*, 82nd edn., edited by D.R. Lide (CRC Press, Florida, 2001)
25. M. Godefroid, C. Fröse Fischer, P. Jönsson, *J. Phys. B* **34**, 1079 (2001)
26. C. Fröse Fischer, M. Saporov, G. Gaigalas, M. Godefroid, *At. Data Nucl. Data Tables* **70**, 119 (1998)